Institut za nuklearne
nauke Vinča

Highlights

- $Li_{1.8}Na_{0.2}TiO_3:Mn^{4+}$ was synthesized by the solid-state reaction method in C2/c structure.

- The material was used as a probe for the lifetime-based luminescence thermometry.

- Mn^{4+} emits around 679 nm due to of $^2E_g \rightarrow {}^4A_{2g}$ spin forbidden electron transition.

- The material exhibits a large value of relative sensitivity (2.6% K^{-1}@340 K).

- Excellent Mn^{4+} emission repeatability with temperature resolution of 0.1 K.

Li$_{1.8}$Na$_{0.2}$TiO$_3$:Mn^{4+}: the highly sensitive probe for the low-temperature lifetime-based luminescence thermometry

Milica Sekulić[1], Zoran Ristić[1], Bojana Milićević[1,2], Željka Antić,[1] Vesna Đorđević[1*], Miroslav D. Dramićanin[1*]

[1]*University of Belgrade, Vinča Institute of Nuclear Sciences, PO Box 522, 11001 Belgrade, Serbia,*

[2]*Sun Yat-Sen University, No. 135, Xingang Xi Road, Guangzhou, 510275, P. R. China*

[*]Corresponding author emails: dramican@vinca.rs (M.D. Dramićanin) vesipka@vinca.rs (V. Đorđević)

Abstract:

In this work, the potential of Li$_{1.8}$Na$_{0.2}$TiO$_3$:Mn^{4+} for the lifetime-based luminescence thermometry is assessed. The material is prepared by the solid-state reaction of Li$_2$CO$_3$, Na$_2$CO$_3$, and nanostructured TiO$_2$ at 800°C, and its monoclinic structure (space group C2/c) is confirmed by X-ray diffraction analysis. In this host, Mn^{4+} provides strong absorption around 330 nm and 500 nm due to ^{4}A$_{2g}$ → ^{4}T$_{1g}$ and ^{4}A$_{2g}$ → ^{4}T$_{2g}$ electric dipole forbidden and spin-allowed electron transitions, respectively, and emits around 679 nm on account of ^{2}E$_g$ → ^{4}A$_{2g}$ spin forbidden electron transition. Temperature dependences of emission intensity and emission decay are measured over the 10–350 K range. Due to the low value of energy of ^{4}T$_{2g}$ level (20000 cm^{-1}), the strong emission quenching starts at low-temperatures which favors the use of this material for the luminescence thermometry. It is demonstrated that the quite large value of relative sensitivity (2.6% K^{-1}@340 K) facilitates temperature measurements with temperature resolution better than 0.1 K, and with the excellent repeatability.

Keywords: Luminescence thermometry; phosphor; Mn^{4+}; Lithium titanium oxide; Temperature dependence of emission; Temperature sensors

1. Introduction

Much effort is directed to the development of optical methods for temperature measurements these days. Although temperature is one of the most commonly measured physical properties, accurate temperature measurements are still to be realized in some emerging environments, such as at the nanoscale or intracellular environments. [1,2]. Luminescence is a temperature dependent phenomenon. Thus, many materials can be used as luminescence thermometry probes by exploiting temperature induced changes in their excitation and emission band positions and bandwidths [3–5], emission band intensity [6–9], ratio of intensities of two emission bands [10–19], and excited-state lifetimes [20–32].

Temperature readings from the variations the emission intensity ratios and excited-state lifetimes are utilized much more frequently than from other luminescence features since these methods are self-referencing and are robust in respect to fluctuations in excitation power, detector sensitivity, and concentration of the probe material [33].

Luminescence thermometry based on excited-state lifetime measurements requires monitoring of just one emission band and, therefore, has an advantage over emission intensity ratiometric method which needs monitoring of two distinctively separated emissions to achieve self-referencing. On the other hand, excited-state lifetime methods show lower temperature sensitivities than ratiometric methods. However, measurements of temporal emission changes are much more accurate than emission intensity measurements, and lower measurement uncertainties compensate for lower sensitivities so that lifetime methods with sensitive probes may provide better temperature resolution than ratiometric methods [17]. Materials of choice are usually lanthanide and transition metal activated phosphors because they exhibit large emission quantum efficiencies, are chemically and thermally stable, show no photobleaching, and have excited state lifetimes on order of μs and longer. Lanthanide activated phosphors are suitable for high-temperature measurements since their lifetime has an almost constant value in the low- and mid-temperature ranges. In transition metal activated phosphors, excited state lifetime starts to decrease at lower temperatures than in lanthanide phosphors so that luminescence thermometry can be employed from cryogenic temperatures to room temperatures or even slightly higher. Good candidates are Mn^{4+} activated oxides since these phosphors have a strong excitation band in the blue spectral region so that emissions can be excited with a cheap LED source, and have low value of $^{4}T_{2g}$ energy level which favors emission quenching even at low temperatures. Also, emission from ^{2}Eg level in the 650-730 nm range is less affected by the environmental (parasitic) luminescence than shorter-wavelength emissions. The materials have optimal values of lifetimes (few tens of μs to ms) which provide good temporal resolution of measurements (lifetimes greater than 1 ms are not suitable for fast measurements).

Here, we aimed to investigate the potential of $Li_{1.8}Na_{0.2}TiO_3$:Mn^{4+} as a lifetime-based luminescence thermometry probe since the recent report on Li_2TiO_3:Mn^{4+} [34] showed that it provides favorable luminescence properties for this application.

2. Experimental section
2.1. Synthesis

$Li_{1.8}Na_{0.2}TiO_3$:0.5%Mn^{4+} sample was prepared by traditional solid state synthesis in air. Li_2CO_3 (Alfa Aesar, 99 %), Na_2CO_3 (Alfa Aesar, 98 %), TiO_2 (nanostructured anatase TiO_2 prepared by titanium isopropoxide hydrolysis [35]) and MnO_2 (Alfa Aesar, 98 %) were used as starting materials. The precursor powder was grounded in pestle and mortar with ethyl alcohol as a binder for 2 h. Then the mixture is gradually heated to 670°C and calcined for 3 h. The sample was cold-pressed under 700 MPa pressure and then sintered for 72 h at 800 °C. The pellets were cooled in furnace to room temperature to form pure-phase.

2.2. Instruments and measurements

X-ray diffraction (XRD) measurements were performed on a Rigaku SmartLab system operating with Cu Kα radiation (30 mA, 40 kV) in the 2θ range from 10° to 90°. Optical Parametric Oscillator (EXPLA NT342) was used as an excitation source for luminescence measurements and emissions were recorded using FHR1000 monochromator (Horiba Jobin Yvon) and iCCD camera (Horiba Jobin Yvon 3771). Mn^{4+} emission decay times were measured over the 10–350 K temperature range using a closed-cycle cryostat (Advanced Research System

DE202-AE) equipped with a Lakeshore model 331 controller. Diffuse reflectance measurements were performed with Shimadzu UV-2600 (Shimadzu Corporation, Tokyo, Japan) spectrophotometer equipped with an integrated sphere (ISR-2600).

3. Results and Discussions

This material has a monoclinic structure (space group C2/c) [36,37] as evidenced by the synthesized powder X-ray diffraction pattern shown in Fig. 1 (diffractions are indexed according to ICDD: 01-077-8280).
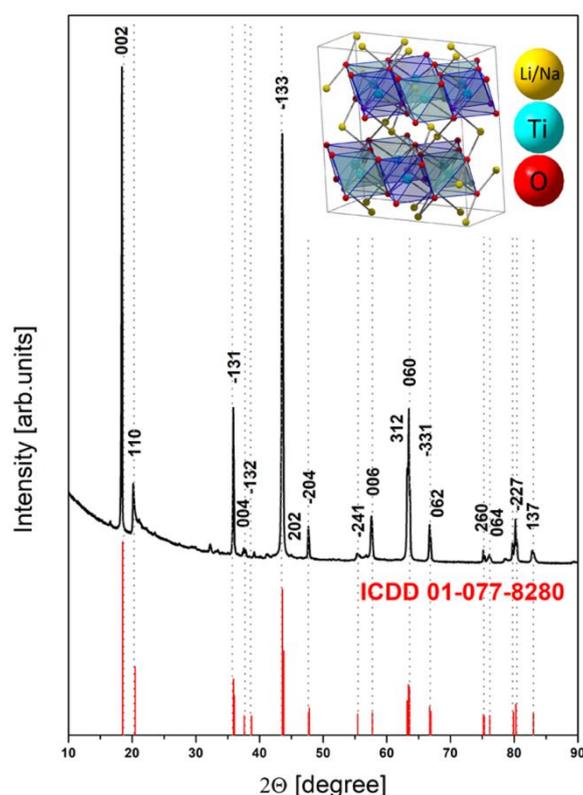

Figure 1. XRD pattern of $Li_{1.8}Na_{0.2}TiO_3$:0.5%Mn powder indexed according to ICDD: 01-077-8280; inset illustrates the crystal structure of $Li_{1.8}Na_{0.2}TiO_3$

Ti^{4+} ions are situated in two nearly identical crystallographic sites (4e symmetry), and in both of them Ti is in octahedral oxygen coordination.

Mn^{4+} substitutes Ti^{4+} in $Li_{1.8}Na_{0.2}TiO_3$, so that local Ti site symmetries are reflected in the splitting of the Mn^{4+} energy levels and diffuse reflection and photoluminescence emission spectra, Fig. 2.
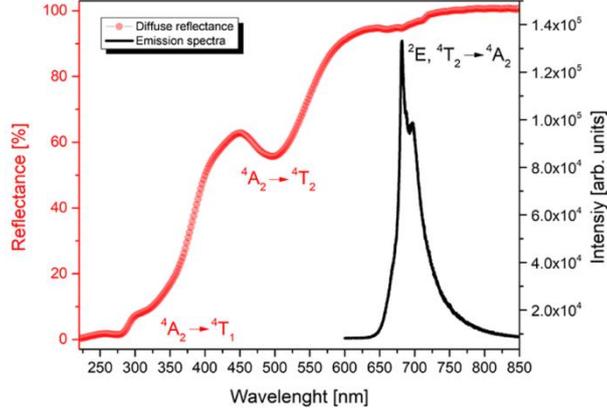
Figure 2. Room temperature diffuse reflectance (red symbols) and emission (black line; excited by 490 nm radiation) spectra of $Li_{1.8}Na_{0.2}TiO_3$:0.5%Mn.

The diffuse reflection spectrum, Fig. 2 (red symbols), of $Li_{1.8}Na_{0.2}TiO_3$:Mn^{4+} is characterized by absorptions of the O^{2-}—Mn^{4+} and O^{2-}—Ti^{4+} charge transfer bands (at wavelengths < 300 nm) and the Mn^{4+} broad intra-configurational (3d→3d) absorption bands originating from $^4A_{2g}$ → $^4T_{2g}$ (around 500 nm) and $^4A_{2g}$ → $^4T_{1g}$ (around 330 nm) electric dipole (parity) forbidden and spin-allowed electron transitions. The emission spectrum, Fig. 2 (black line), is due to the ^2E_g → $^4A_{2g}$ spin forbidden electron transition (around 679 nm), with the contribution of the associated vibronic sidebands and some contribution from the $^2T_{1g}$ → $^4A_{2g}$ spin-allowed transition.

The temperature dependence of Mn^{4+} emission is recorded over the 10–350 K range is shown in Fig. 3. At low temperatures, the non-radiative deexcitation rate is negligible so that emission intensity and lifetime vary only slightly with temperature (due to variation of the radiative rate). At higher temperatures, both the emission intensity (Fig. 3(a)) and emission lifetime (Fig. 3(b)) are temperature quenched through the $^4T_{2g}$ level [38].
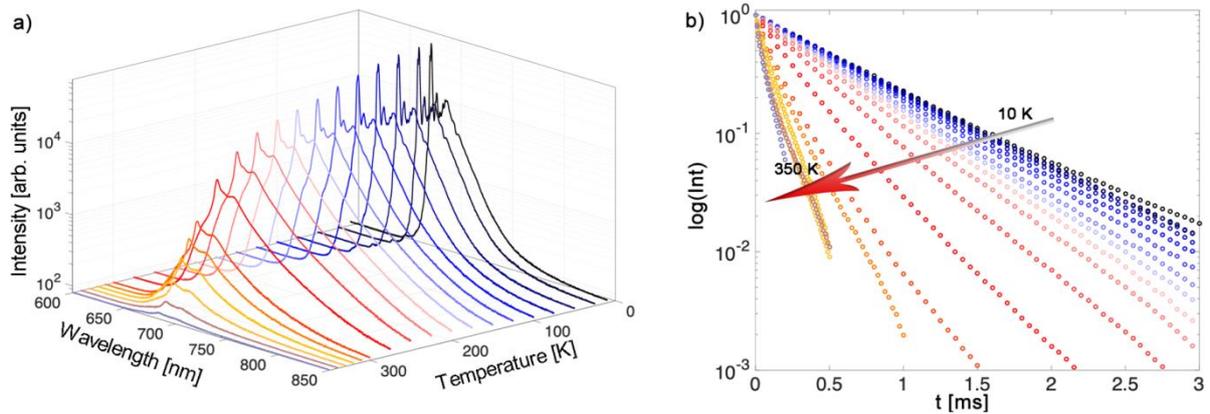

Figure 3. The temperature dependence of $Li_{1.8}Na_{0.2}TiO_3$:0.5%Mn^{4+} emission in the 10–350 K range: (a) emission spectra measured with 490 nm excitation, (b) decay of 679 nm emissions.

The temperature dependence of the excited state lifetime can be described by the following formula [38]:

$$\tau(T) = \frac{\tau_R(0)\cdot\tanh{(h\nu/2k_BT)}}{1+(\tau_R(0)\cdot\tanh{(h\nu/2k_BT)}/\tau_{NR})\cdot\exp{(-\Delta E/k_BT)}}, \tag{1}$$

where $\tau_R(0)$ is the radiative lifetime at $T = 0$ K, $k_B = 0.69503476$ cm^{-1}/K is the Boltzmann constant, $h\nu$ is the average energy of phonons coupled to the $^2E_g \rightarrow {}^4A_{2g}$ transition, $1/\tau_{NR}$ is the non-radiative decay rate, ΔE is the activation energy of the cross-over process via the $^4T_{2g}$ level, and T represents the temperature. Figure 4(a) shows the experimental data of the lifetime dependence on temperature (symbols) and the fit of Eq. (1) to experimental data (red line; $\tau_R(0) = 0.6858$ ms, $h\nu = 257.6$ cm^{-1}, $1/\tau_{NR} = 6 \cdot 10^8$ s^{-1}, $\Delta E = 2574$ cm^{-1}, R^2=0.998).
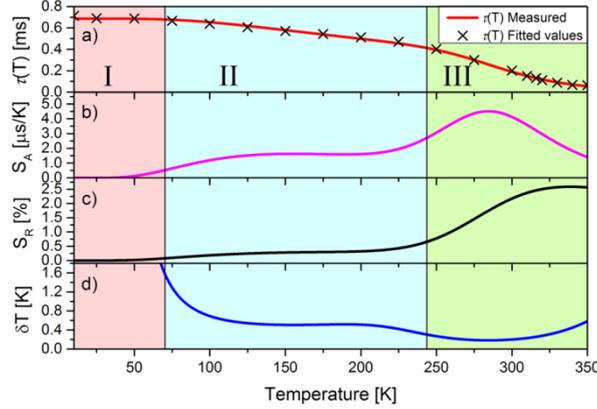

Figure 4. (a) The temperature dependence of the Mn^{4+} emission lifetime (symbols); the red line represent fit to Eq. (1), (b,c) the absolute and relative sensitivity respectively, and (d) the temperature resolution of thermometry.

One can observe three temperature regions in which lifetimes change differently with increase in temperature. In the first one, where temperature is lower than 75 K, the lifetime is constant and equals the value of $\tau_R(0)$. For temperatures between 75 and 230 K (the second temperature region), the lifetime decreases because of an increased probability of phonon induced transitions between the Mn^{4+} ^2E_g and $^4A_{2g}$ states. In the third region, for temperatures larger than 230 K, the lifetime strongly decreases due to an increase in the rate nonradiative processes. The applicability of this material for luminescence thermometry can be assessed from the change of the lifetime with temperature, i.e. from the absolute (S_a) or relative (S_R) sensitivity of the measurement, which can be derived from the Eq. (1) as:

$$S_a(T)\ [s \cdot K^{-1}] = \frac{d\tau(T)}{dT}$$
$$= -\frac{\tau_R(0)\cdot\tanh{(h\nu/2k_BT)}}{k_BT^2}\frac{h\nu/(2\cdot\sinh{(h\nu/2k_BT)}\cdot\cosh{(h\nu/2k_BT)}) + \Delta E \cdot (\tau_R(0)\cdot\tanh{(h\nu/2k_BT)}/\tau_{NR})\cdot\exp{(-\Delta E/k_BT)}}{[1 + (\tau_R(0)\cdot\tanh{(h\nu/2k_BT)}/\tau_{NR})\cdot\exp{(-\Delta E/k_BT)}]^2},$$

$$S_R\ (T)\ [\%] = \left|\frac{1}{\tau(T)}\cdot\frac{d\tau(T)}{dT}\right|\cdot 100\% =$$

$$= \left|\frac{1}{k_BT^2}\frac{h\nu/(2\cdot\sinh{(h\nu/2k_BT)}\cdot\cosh{(h\nu/2k_BT)}) + \Delta E\cdot(\tau_R(0)\cdot\tanh{(h\nu/2k_BT)}/\tau_{NR})\cdot\exp{(-\Delta E/k_BT)}}{1+(\tau_R(0)\cdot\tanh{(h\nu/2k_BT)}/\tau_{NR})\cdot\exp{(-\Delta E/k_BT)}}\right|\cdot 100\% \tag{2}$$

are given in Figs. 4(b) and (c). The onset of applicability is at 75 K, and the relative sensitivity increases in value with a temperature increase. In the first temperature region, the relative sensitivity has a moderate value, in the 0.1–0.5 %K^{-1} range. For temperatures larger than 230 K, in the third temperature region, the relative sensitivity is a quite high, with maximum value

of 2.59 %K^{-1} at 340 K. Such high sensitivity facilitates measurement with temperature resolution which is among the highest ever reported for the luminescence thermometry, Fig. 4(c). The temperature resolution is calculated from the uncertainty in lifetime measurement, Fig. 5(a), as $\delta T(T) = \sigma/S_a$, where $\sigma = 0.8228$ μs represents the value of measurement uncertainty. It has good values (from 1 to 0.2 K) in the 75–230 K temperature range, and exceptional value 0.1K and lower around room temperatures, third region in Fig. 4(c). Cycles of lifetime measurements were performed between two temperatures, see Fig. 5(b), and an excellent repeatability was observed.
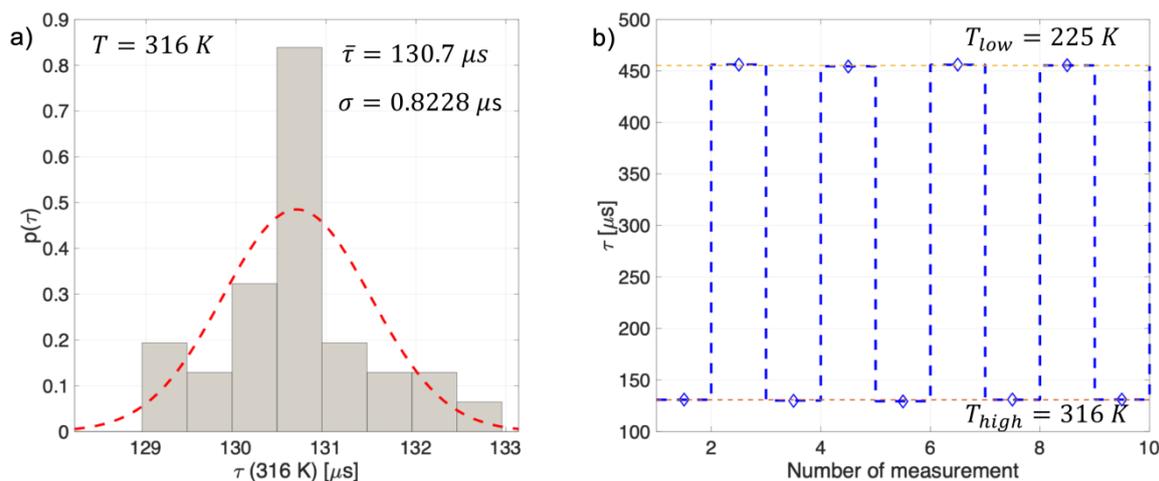

Figure 5. (a) The distribution of lifetime values measured at 316 K, (b) the repeatability of lifetime measurements demonstrated by measuring lifetime while cycling between two temperatures.

Conclusion

Li$_{1.8}$Na$_{0.2}$TiO$_3$:Mn^{4+} probe for the lifetime-based luminescence thermometry provides high-sensitivity temperature readings for temperatures higher than 75 K with a quite high temperature resolution, better than 0.1 K around room temperature. This probe can be excited by the blue light and emits in the deep-red spectral region (because of the strong nephelauxetic effect in oxides) where the contribution of parasitic background luminescence is minimal. The strong quenching of emissions at relatively low temperatures is a consequence of the low energy value of ^{4}T$_{2g}$ level which facilitates the low-energy activation ($\Delta E = 2574$ cm^{-1}) of the quenching process via the cross-over from ^{2}E$_g$ to ^{4}T$_{2g}$ and finally to the ground state. As for the most of lanthanide and transition metal activated phosphors, the repeatability of measurements is almost perfect. The presented results show that Li$_{1.8}$Na$_{0.2}$TiO$_3$:0.5%Mn^{4+} is a suitable candidate for the development of accurate and self-referencing luminescent temperature sensors. The results also suggest that it is possible to engineer the lifetime-based Mn^{4+} activated luminescent probes for targeted applications and temperature ranges by selecting host materials of suitable energy of the ^{4}T$_{2g}$ state and the energy of phonon coupling to the ^{2}E$_g \rightarrow {}^4$A$_{2g}$ transition.

References:

[1] D. Ross-Pinnock, P.G. Maropoulos, Review of Industrial Temperature Measurement Technologies and Research Priorities for the Thermal Characterisation Of The Factories Of The Future, Proc. Inst. Mech. Eng. Part B J. Eng. Manuf. 230 (2016) 793–806. https://doi.org/10.1177/0954405414567929

[2] M. Dramićanin, Introduction to Measurements of Temperature, in: Luminescence Thermometry, Woodhead Publishing, 2018, pp. 1–12. https://doi.org/10.1016/B978-0-08-102029-6.00001-4.

[3] H. Kusama, O. J. Sovers, T. Yoshioka, Line shift method for phosphor temperature measurements, Jpn. J. Appl. Phys. 15 (1976) 2349–2358. https://doi.org/10.1143/JJAP.15.2349

[4] R. Liang, R. Tian, W. Shi, Z. Liu, D. Yan, M. Wei, D.G. Evans, X. Duan, A temperature sensor based on CdTe quantum dots–layered double hydroxide ultrathin films via layer-by-layer assembly, Chem. Commun. 49 (2013) 969–971. https://doi.org/10.1039/C2CC37553B

[5] H. Peng, H. Song, B. Chen, J. Wang, S. Lu, X. Kong, J. Zhang, Temperature dependence of luminescent spectra and dynamics in nanocrystalline $Y_2O_3:Eu^{3+}$, J. Chem. Phys. 118 (2003) 3277–3282. https://doi.org/10.1063/1.1538181

[6] G.W. Walker, V.C. Sundar, C.M. Rudzinski, A.W. Wun, M.G. Bawendi, D.G. Nocera, Quantum-dot optical temperature probes, Appl. Phys. Lett. 83 (2003) 3555–3557. https://doi.org/ 10.1063/1.1620686

[7] D. Jaque, F. Vetrone. Luminescence Nanothermometry, Nanoscale 4 (2012) 4301–4326. https://doi.org/10.1039/C2NR30764B

[8] V. Lojpur, M.G. Nikolić, D. Jovanović, M. Medić, Ž. Antić, M.D. Dramićanin. Luminescence thermometry with $Zn_2SiO_4:Mn^{2+}$ powder. Appl Phys Lett 103 (2013) 141912. https://doi.org/10.1063/1.4824208

[9] S. Uchiyama, N. Kawai, A.P. de Silva, K. Iwai, Fluorescent polymeric and logic gate with temperature and pH as inputs, J. Am. Chem. Soc. 126 (2004) 3032–3033. https://doi.org/10.1021/ja039697p

[10] S. Zhou, S. Jiang, X. Wei, Y. Chen, C. Duan, M. Yin, Optical thermometry based on upconversion luminescence in Yb^{3+}/Ho^{3+} co-doped $NaLuF_4$, J. Alloys Comp. 588 (2014) 654–657. https://doi.org/10.1016/j.jallcom.2013.11.132

[11] Z. Feng, L. Lin, Z. Wang, Z. Zheng, Low temperature sensing behavior of upconversion luminescence in Er^{3+}/Yb^{3+} codoped PLZT transparent ceramic, Opt. Commun. 399 (2017) 40–44. http://dx.doi.org/10.1016/j.optcom.2017.04.051

[12] G. Chen, R. Lei, F. Huang, H. Wang, S. Zhao, S. Xu, Optical temperature sensing behavior of $Er^{3+}/Yb^{3+}/Tm^{3+}:Y_2O_3$ nanoparticles based on thermally and non-thermally

coupled levels, Opt. Commun. 407 (2018) 57–62. http://dx.doi.org/10.1016/j.optcom.2017.09.014

[13]   L. Yu, L. Ye, R. Bao, X. Zhang, L. Wang, Sensitivity-enhanced Tm^{3+}/Yb^{3+} co-doped YAG single crystal optical fiber thermometry based on upconversion emissions, Opt. Commun. 410 (2018) 632–636. https://doi.org/10.1016/j.optcom.2017.10.075

[14]   M.D. Dramićanin, Sensing temperature via downshifting emissions of lanthanide-doped metal oxides and salts. A review, Methods Appl. Fluoresc. 4 (2016) 042001. https://doi.org/10.1088/2050-6120/4/4/042001

[15]   T.V. Gavrilović, D.J. Jovanović, V. Lojpur, M.D. Dramićanin, Multifunctional Eu^{3+}- and Er^{3+}/Yb^{3+}-doped $GdVO_4$ nanoparticles synthesized by reverse micelle Method, Sci. Rep. 4 (2014) 4209. https://doi.org/10.1038/srep04209

[16]   D. Chen, S. Liu, Y. Zhou, Z. Wan, P. Huang, Z. Ji, Dual-activator luminescence of RE/TM: $Y_3Al_5O_{12}$ (RE=Eu^{3+}, Tb^{3+}, Dy^{3+}; TM=Mn^{4+}, Cr^{3+}) phosphors for self-referencing optical thermometry, J. Mater. Chem. C 4 (2016) 9044–9051. https://doi.org/10.1039/C6TC02934E

[17]   M.G. Nikolić, Ž. Antić, S. Ćulubrk, J.M. Nedeljković, M.D. Dramićanin. Temperature sensing with Eu^{3+} doped TiO_2 nanoparticles. Sensors Actuators B Chem. 201 (2014) 46–50. https://doi.org/10.1016/j.snb.2014.04.108

[18]   M.D. Dramićanin, Ž. Antić, S. Ćulubrk, S.P. Ahrenkiel, J.M. Nedeljković, Self-referenced luminescence thermometry with Sm^{3+} doped TiO_2 nanoparticles, Nanotechnology 25 (2014) 485501, https://doi.org/10.1088/0957-4484/25/48/485501

[19]   Ł. Marciniak, A. Bednarkiewicz, M. Stefanski, R. Tomala, D. Hreniak, W. Strek, Near infrared absorbing near infrared emitting highly-sensitive luminescent nanothermometer based on Nd^{3+} to Yb^{3+} energy transfer, Phys. Chem. Chem. Phys. 17 (2015) 24315–24321. https://doi.org/10.1039/C5CP03861H

[20]   V. Lojpur, Ž. Antić, M.D. Dramićanin, Temperature sensing from the emission rise times of Eu^{3+} in SrY_2O_4, Phys. Chem. Chem. Phys. 16 (2014) 25636–25641. https://doi.org/10.1039/C4CP04141K

[21]   P. Haro-González, L. Martínez-Maestro, I.R. Martín, J. García-Solé, D. Jaque, High-sensitivity fluorescence lifetime thermal sensing based on CdTe quantum dots, Small 8 (2012) 2652–2658. https://doi.org/10.1002/smll.201102736

[22]   D. Seto, R. Nikka, S. Nishio, Y. Taguchi, T. Saiki, Y. Nagasaka, Nanoscale optical thermometry using a time-correlated single-photon counting in an illumination-collection mode, Appl. Phys. Lett. 110 (2017) 033109. https://doi.org/10.1063/1.4974451

[23]   F. Zhao, J. Kim, Study on the lifetime decay of quantum dots as a function of temperature, J Nanosci. Nanotechno. 14 (2014) 5947–5950. https://doi.org/10.1166/jnn.2014.8813

[24]   S.W. Allison, G.T. Gillies, A.J. Rondinone, M.R. Cates, Nanoscale thermometry via the fluorescence of YAG:Ce phosphor particles: measurements from 7 to 77°C, Nanotechnology 14 (2003) 859–863. https://doi.org/10.1088/0957-4484/14/8/304

[25]   F. Li, J. Cai, F.F. Chi, Y. Chen, C. Duan, M. Yin, Investigation of luminescence from LuAG: Mn^{4+} for physiological temperature sensing, Opt. Mater. 66 (2017) 447–452. https://doi.org/10.1016/j.optmat.2017.02.054

[26] H. Aizawa, H. Uchiyama, T. Katsumata, S. Komuro, T. Morikawa, H. Ishizaw, E. Toba, Fibre-optic thermometer using sensor materials with long fluorescence lifetime, Meas. Sci. Technol. 15 (2004) 1484–1489. https://doi.org/10.1088/0957-0233/15/8/009

[27] J.I. Eldridge, M. D. Chambers, Fiber optic thermometer using Cr-doped $GdAlO_3$ broadband emission decay, Meas. Sci. Technol. 26 (2015) 95202. https://doi.org/10.1088/0957-0233/26/9/095202

[28] K.T.V. Grattan, A.W. Palmer, Infrared fluorescence ''decay-time'' temperature sensor, Rev. Sci. Instrum. 56 (1985) 1784–1787. https://doi.org/10.1063/1.1138094

[29] Z.P. Cai, L. Xiao, H.Y. Xu, M. Mortier, Point Temperature sensor based on green decay in an Er:ZBLALiP microsphere, J. Lumin. 129 (2009) 1994–1996. https://doi.org/10.1016/j.jlumin.2009.04.039

[30] X. Wang, Y. Wang, Y. Bu, X. Yan, J. Wang, P. Cai, T. Vu, H. J. Seo, Improving optical temperature sensing performance of Er^{3+} Doped Y_2O_3 microtubes via co-doping and controlling excitation power, Sci. Rep. 7 (2017) 1–9. https://doi.org/10.1038/s41598-017-00838-w

[31] L. Marciniak, K. Trejgis, Luminescence lifetime thermometry with Mn^{3+}–Mn^{4+} co-doped nanocrystals, J. Mater. Chem. C 6 (2018) 7092–7100, https://doi.org/10.1039/C8TC01981A

[32] Y. Zhou, B. Yan, Ratiometric detection of temperature using responsive dual-emissive MOF hybrids, J. Mater. Chem. C, 3 (2015) 9353–9358. https://doi.org/10.1039/C5TC02004B

[33] M. Dramićanin, Schemes for Temperature Read-Out From Luminescence, in: Luminescence Thermometry, Woodhead Publishing, 2018, pp. 63–83. https://doi.org/10.1016/B978-0-08-102029-6.00004-X.

[34] F. Yang, L. Qiao, H. Ren, F. Yan, Luminescence analysis of Mn^{4+},Zn^{2+}: Li_2TiO_3 red phosphors, J. Lumin. 194 (2018) 179–184. https://doi.org/10.1016/j.jlumin.2017.10.035

[35] B. O'Regan, J. Moser, M. Anderson, M. Gratzel, Vectorial electron injection into transparent semiconductor membranes and electric field effects on the dynamics of light-induced charge separation, J. Phys. Chem. 94 (1990) 8720–8726. https://doi.org/10.1021/j100387a017

[36] J. F. Dorrian, R. E. Newnham, Refinement of the structure of Li_2TiO_3, Mater. Res. Bull. 4 (1969) 179–183. https://doi.org/10.1016/0025-5408(69)90054-3

[37] K. Kataoka, Y. Takahashi, N. Kijima, H. Nagai, J. Akimoto, Y. Idemoto, K. Ohshima, Crystal growth and structure refinement of monoclinic Li_2TiO_3, Mater. Res. Bull. 44 (2009) 168–172. https://doi.org/10.1016/j.materresbull.2008.03.015

[38] T. Senden, R. J. A. van Dijk-Moes and A. Meijerink, Quenching of the red Mn^{4+} luminescence in Mn^{4+}-doped fluoride LED phosphors, Light Sci. Appl., 7 (2018) 8. https://doi.org/10.1038/s41377-018-0013-1